sustainability

MDPI

Article

Sustainability of Discontinuously Supported Slopes in Temporary Shallow Excavations for Building Construction: A Stability Analysis Procedure

Miguel A. Millán *, David Mencías-Carrizosa and Alejandro Calle

Physics and Building Structures Department, Universidad Politécnica de Madrid, ETS Arquitectura, Avda. Juan de Herrera n°4, 28040 Madrid, Spain; d.mencias@upm.es (D.M.-C.); alejandro.calle@upm.es (A.C.)
* Correspondence: miguelangel.millan@upm.es

Abstract: Sustainable building construction requires a design process that ensures long-term structural durability and minimizes risks of failure or damage during construction and throughout the structure's service life. One critical aspect of this process is the excavation of simple basements, which often requires discontinuously supported excavation (shielding) when soil stability is compromised, or nearby buildings or infrastructure are at risk. Despite the apparent simplicity of this technique, the lack of a standardized procedure to verify the safety of excavated slopes frequently leads to accidents and damage to adjacent structures. This research introduces a methodology for assessing the safety of discontinuously supported excavations. The proposed method involves a series of calculations based on the Finite Element Method (FEM) to develop a stability chart. Currently, no established approach exists to address this complex three-dimensional problem. The models used are characterized by the slope height and the width between supports. The soil is modeled as elastoplastic, following the Mohr–Coulomb failure criterion, with parameters including the friction angle and the cohesive strength. A comprehensive set of simulations is conducted for various heights, widths, and friction angles to determine the minimum cohesive strength required to achieve a specific safety factor. All results are appropriately non-dimensionalized to generate stability charts, which provide an accessible tool for assessing the stability of discontinuously supported slope configurations with a given width between shields.

Keywords: discontinuously supported slope; sustainable excavation; building construction; slope stability

Citation: Millán, M.A.; Mencías-Carrizosa, D.; Calle, A. Sustainability of Discontinuously Supported Slopes in Temporary Shallow Excavations for Building Construction: A Stability Analysis Procedure. *Sustainability* **2024**, *16*, 10393. https://doi.org/10.3390/su162310393

Academic Editors: Moussa Leblouba, Balaji PS, Muhammad Rahman, Brabha Nagaratnam and Keerthan Poologanathan

Received: 30 October 2024
Revised: 20 November 2024
Accepted: 24 November 2024
Published: 27 November 2024

1. Introduction

The calculation of slope stability in building construction is intrinsically linked to sustainability as it involves the assessment and implementation of measures that ensure the stability and safety of the excavation slopes, preventing the risk of human harm and damage to the surrounding buildings and infrastructures. Safe excavation practices, especially in urban areas, support sustainable retaining structures by reducing the environmental impact on surrounding terrain and adjacent buildings, and by improving economic efficiency through optimized resource use, reduced auxiliary equipment needs, and faster project completion. Additionally, it carries social benefits by minimizing risks to nearby structures (especially those that are more vulnerable or of lower construction quality), which minimizes the likelihood of extensive and costly future repairs, ultimately fostering a more resilient and sustainable built environment.

Technical codes do not usually include a procedure to check the stability of shallow excavations when they are discontinuously supported, either by shielding in trenched excavations or by shores or berms in open excavations. These supporting procedures are used in urban excavations for one-level basements when the depth or the location (nearby buildings) of the cut needed to build the retaining wall makes the allowable slope impractical. The existing specific references on construction with discontinuous shielding

or berms only briefly address the problem as in Spain with the Technological Codes of the Ministry of Housing [1] and internationally, for example, with the BS 6031:1981 [2] "Code of Practice for Earthworks" standard or the DIN 4124:2012-01 [3] "Excavations and trenches—Slopes, planking and strutting breadths of working spaces".

Despite its frequent use, there are no widely accepted references or standards for designing and verifying discontinuously supported slopes, unlike for homogeneous slopes, which have established methods, such as the Taylor or Hoek and Bray charts, or two-dimensional calculations using the Bishop method, finite elements, or finite differences. The primary challenge in developing standardized guidelines lies in the three-dimensional nature of the problem, which makes it difficult to address it in a general way without using numerical models. Additionally, because it is not considered a significant geotechnical issue, it has not received much attention from researchers, despite being a well-known cause of accidents and damage to nearby buildings.

Construction safety finally relies on the general guidelines for continuous slopes and trench excavations, as well as on the constructor's experience and good judgment. While these guidelines provide a reference for safety, they correspond to a less stable configuration than discontinuous-supported slopes. Thus, these guidelines do not permit the vertical slopes necessary for constructing basement walls, except for a limited range of soil types. Consequently, when vertical excavations are required, the constructor must rely on their previous experience, as there are no technical procedures to support their decisions. Therefore, it is essential to provide the technical community with a method for analyzing the stability of discontinuous-supported slopes. The use of shield-supported and berm-supported sub-vertical excavations continues to be a common strategy in shallow urban excavations when a uniform slope does not achieve enough safety and certain conditions are met. An image of the problem is presented in Figure 1, showing the construction procedure to build a series of retaining walls between supporting shields, section by section, around the site perimeter. Figure 1a shows the building of a retaining wall using shielding supported by struts leaning on the already excavated center. The subfigure on the left shows two consecutive shields placed laterally at the unsupported slope zone where a retaining wall will be constructed, as shown in the subfigure on the right. Similarly, Figure 1b shows shielding in a trench, leaving a center usually called "dumpling" to be removed after the completion of the retaining walls. Each shield is supported by an additional shield on the opposite slope of the trench.

However, despite its frequent use, there is no extensive and contrasted reference available that allows its design and verification similarly as is done in the usual homogeneous slopes, either by charts such as those of Taylor or Hoek and Bray or two-dimensional numerical calculation with the Bishop method, finite elements or finite differences, among others (as described by Rotaru et al. [4]). The difficulty with calculating the stability of slopes supported by berms lies in the fact that it is a three-dimensional problem, not admitting any of the simplifications that allow it to be reduced to a two-dimensional case and using one of the methods mentioned above.

Many authors have addressed the three-dimensional analysis of slope stability using limit equilibrium methods, which can be followed in the review paper by Azarafza et al. [5]. However, these methods focus on a general 3D stability problem and were not applied to solve the present discontinuously supported slope.

Hisham [6,7] presented the study of a 3D slope with translational failure that may be used to represent a vertical slope supported by discontinuous berms. Similarly, Zhang et al. [8] analyzed the stability of 3D slopes assuming different angles in turning corners, considered in the plan view, which also resembled the problem of a bermed excavation when the slope is vertical, being a valuable procedure to address it.

Several authors, such as Ho [9], Nian et al. [10], Griffiths and Marquez [11], and Samadhiya and Chavda [12], among many others, studied the case of a 3D slope, considering a slope between two parallel boundaries and studying the effects of different boundary conditions on the slope's stability. The case is very similar to the case of a slope

discontinuously supported by shields when the inclination angle is vertical. However, none of them studied this specific configuration.

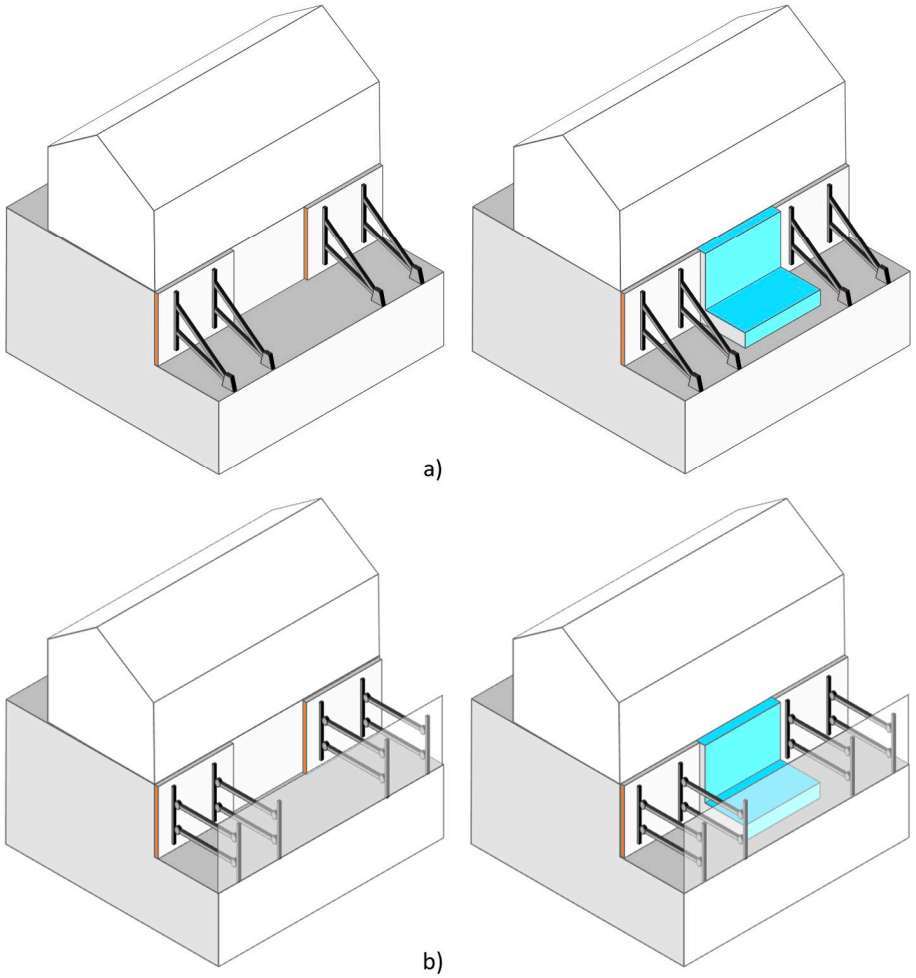

Figure 1. Sketch of a discontinuously supported slope used to build a retaining wall. (**a**) Shields; (**b**) Shields in a trench.

Gourvenec and Powrie [13] addressed a somewhat similar problem to that considered in this research, considering embedded retaining walls supported by discontinuous earth berms, including the effect of the discontinuous support, differently from many other authors that study the so-called bermed excavation (deep excavation supported by an excavation wall and a berm) considering a continuous berm [14–16]. The issue discussed in the referenced research differs from the current study, as it focuses on an embedded retaining wall rather than a traditional one. Additionally, the support mechanism analyzed in the research employs a soil berm instead of a shield, leading to variations in rigidity and performance.

Only recently has some research dealt with the problem, representing the specific conditions of a shallow excavation in building construction. Sabzi and Fakher [17] studied the behavior of a 3D excavation supported by inclined struts adjacent to a building using a 3D FEM model. They centered their research on a prediction of the excavation top and excavation face. Cano et al. [18,19] presented a specific and detailed study on the stability of bermed basement excavations using FEM and proposed design stability charts to address the problem.

The present investigation is oriented towards ensuring the sustainability of shallow excavation in building construction. It provides a model of excavation supported by shields, considering its three-dimensional configuration, and including as main variables the height

of the slope, the open excavation width, and the properties of the ground, represented with a Mohr–Coulomb failure criterion. Stability charts will be obtained from a large number of calculations to allow pre-sizing and verification of the main cases that occur in practice. Providing these stability charts will improve safety in shallow excavation, safeguarding the health and safety of workers while minimizing damage to nearby structures.

2. Materials and Methods

2.1. Problem Definition

This study models two scenarios of discontinuously supported slopes, illustrated in Figure 1a,b. Each configuration shows an open slope with temporary lateral support from shields during the wall's construction. As explained before, these configurations correspond to usual construction procedures in the day-to-day practice of building basements.

The excavation is assumed to be vertical and performed in a uniform soil medium characterized by an elastoplastic behavior, density γ_S, with associated dilatancy, perfect plasticity with linear Mohr–Coulomb failure criterion (with friction angle ϕ and cohesive strength c'). These assumptions are common in practice when evaluating slopes of reduced heights, although the presence of uniform soil is a simplification. Future research will address the consideration of heterogeneous soils. The objective is to analyze the stability of the slope section located between the supported ends, considering the specific conditions that define those supports. The slope geometry, common for all models, is defined (Figure 2) by the unsupported slope width (B) and the slope height (H). Two symmetry planes are included at both ends of the model to reduce its size. The support conditions include rigid support corresponding to rigid shielding, assuming no deformation perpendicular to the sloping plane. Although some deformation of the shielding or the bracing may be expected, null deformation is an acceptable hypothesis since the bracing usually has mechanisms to adapt and restore initial positions.

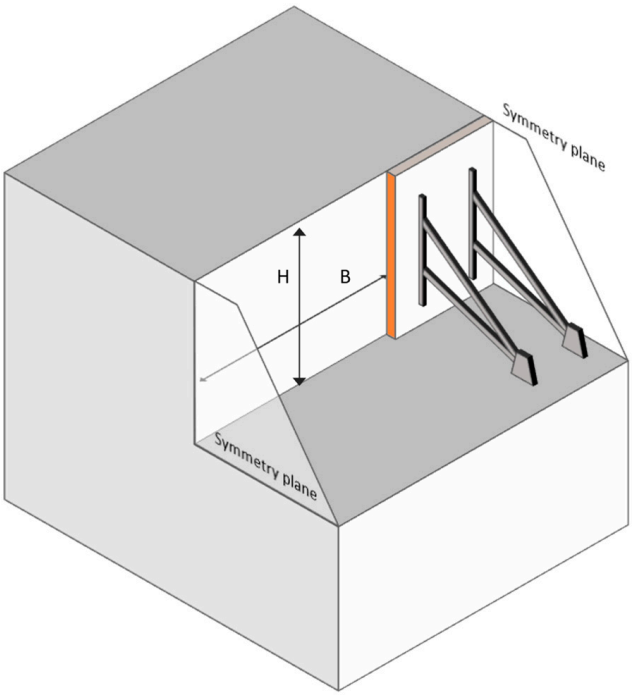

Figure 2. Geometrical definition of the discontinuously supported slope.

Table 1 details the main parameters considered in the evaluation of slope stability. The geomechanical parameters are associated with elastic behavior (E and ν) and the failure criterion (ϕ and c'), as well as the specific soil weight. The geometrical parameters define

the slope geometry (B and H), and the support condition defines the boundary condition at the shielding.

Table 1. Details the main parameters involved in the evaluation of the slope stability.

Parameters Considered for Evaluating Slope Stability	
Geomechanical	Elasticity modulus (E) Poisson coefficient (ν) Specific soil weight (γ) Friction angle (ϕ) Cohesive strength (c')
Geometrical	Slope width (B) Slope height (H)
Support conditions	Non-deformable (shielding)

2.2. Slope Stability Analysis

The usual practice assumes as an established calculation method the so-called Shear Strength Reduction Method [20]. This method uses a resistance reduction factor F that applies to both the friction angle and the cohesion of the terrain, as follows:

$$c'_f = \frac{c'}{F} \tag{1}$$

$$\varphi'_f = \text{arctg}\left(\frac{\text{tg}\phi'}{F}\right) \tag{2}$$

By successively increasing the value of the coefficient F, in such a way that the resistant properties of the terrain decrease until the model does not converge to a solution, the safety factor is defined as the value of F immediately before failure. The method is employed within the finite element method framework, executing a progressive calculation within the same model while systematically decreasing the cohesive strength at each iteration until the software identifies instability in the model.

The number of stability N_s is used to normalize the stability results, dividing the cohesive strength by the gravity vertical stress at the bottom of the slope:

$$N_s = \frac{\gamma \cdot H}{c_a} \tag{3}$$

The stability number N_s represents the ratio between the vertical stress at the toe of the slope, which is the most stressed point in the soil, and the main resistant parameter of the soil (C_u/F). This ratio establishes the importance of stresses in the soil relative to its strength and can be used to compare the response for different soils.

This formulation is expanded to include the influence of surface loads (q) on top of the slope, representing building foundations, and roads adjacent to the excavation, etc. It is supposed to be extended over the top surface of the terrain.

The number of stability N_s is changed, including the stress due to the load q in the vertical stress at the bottom of the slope:

$$N_s = \frac{\gamma \cdot H + q}{c_a} \tag{4}$$

In present research, the ratio $N_s/N_{s\infty}$ is used to normalize the stability number for all the results, being $N_{s\infty}$ the stability number for the 2D slope, corresponding to a slope having infinite width.

2.3. Finite Element Models

A three-dimensional finite element model of the problem is built using the commercial software Abaqus 2017 [21].

The model assumes a uniform soil structure, overlooking potential heterogeneity, which should be investigated in future research.

Unlike the traditional slope stability analysis that can be represented with a two-dimensional model, the studied problem needs a full three-dimensional one because of its discontinuity and the different boundary conditions in the free slope and the supported one.

The model employs symmetrical conditions to minimize the size by representing only half of the domain, as illustrated previously in Figure 2. The assumption of symmetry means that the model is mirrored on both sides, which restricts normal displacement at these symmetry planes (referred to as sliding boundaries). The boundary at the bottom plane is fixed, while the shielded boundary allows for shear displacement only, prohibiting normal displacement. The model represents the free and shielded slopes, as shown in Figure 3.

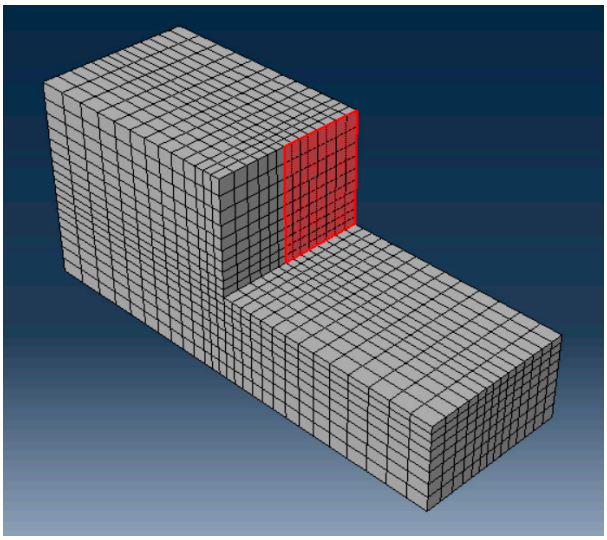

Figure 3. Schematic representation of the numerical model with shielded support (represented by the red area in the figure).

Boundary conditions are properly arranged to represent symmetry and to determine conditions at the extremes consistent with the assumed behavior of the soil. They are detailed in Figure 4 on an elevation and floor plan of the model.

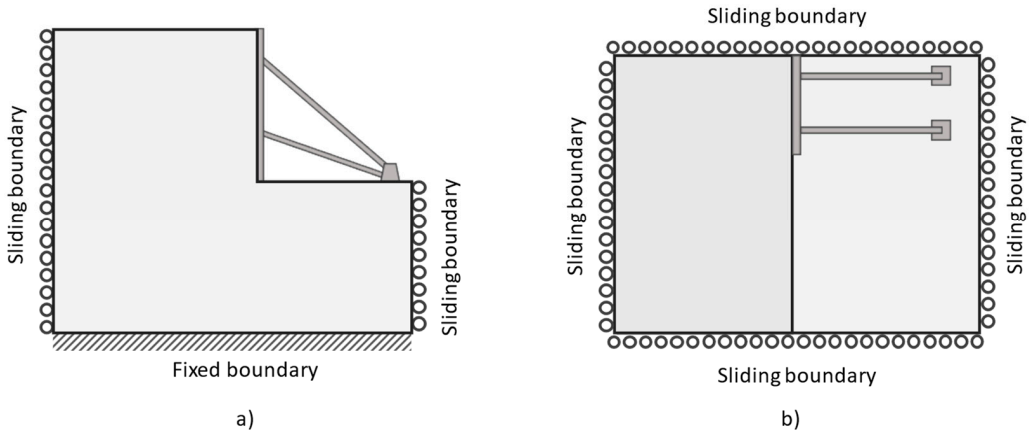

Figure 4. Schematic representation of the numerical model boundary conditions. (**a**) Elevation plan and (**b**) floor plan.

The Mohr–Coulomb (MC) model in Abaqus is different from the traditional MC model [22]. In Abaqus, a smooth flow potential with a hyperbolic shape in the meridional stress plane and a piecewise elliptic shape in the deviatoric stress plane are used. The friction angle and cohesive stress should be defined in the plane of the maximum and minimum principal stresses and then converted to be expressed in the traditional MC plane σ-τ.

The model uses 8-node linear brick-type elements (C3D8R in Abaqus), and 6-node linear triangular prism elements (C3D6 in Abaqus), depending on the model part. The mesh is adapted to have a denser distribution around the high stressed zones. A convergence study is performed to test the accuracy of the results depending on the mesh density, resulting in Figure 5. As can be seen, with a representative size greater than 1/d = 3 (elements with size 0.33 m or smaller), the obtained value of c' (cohesive strength needed to the slope stability) does not change, meaning that no better results of c' can be obtained with finer meshes, making it unnecessary to reduce its size.

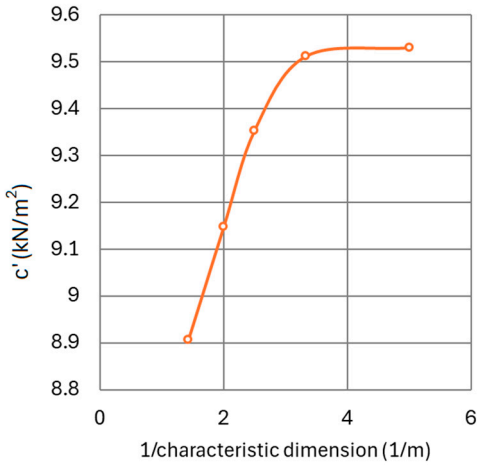

Figure 5. Mesh convergence analysis.

2.4. Case Studies

A sensitivity study of slope stability is performed for different values of the geometrical dimensions and the soil properties. The values adopted in this work for the geomechanical and geometrical parameters are included in Table 2.

Table 2. Case studies for evaluating slope stability.

Geomechanical	Elasticity modulus (E)	200 MPa
	Poisson coefficient (ν)	0.3 (non-dimensional)
	Specific soil weight (γ_S)	20 kN/m^3
	Friction angle (ϕ)	5/10/20/40 (sexagesimal degrees)
	Cohesive strength (c')	Obtained as a result (MPa)
Geometrical	Slope width/height ratio ($B^* = B/H$)	0.25/0.5/1/2/2.5/3/3.5/4 (m/m)
	Shield width	3 m

All the cases considered above are studied for the three different support conditions defined in Table 1. The results obtained are normalized using the ratios N_s/N_∞, where N_∞ is the stability number corresponding to the slope of infinite width, and the geometry using the ratio of the slope width to its height $B^* = B/H$.

The reference model is defined using H = 4 m. Identical results are obtained using a different slope height H if the same B/H ratio is considered, as proved in Figure 6 for H = 10 m and friction angle ϕ' = 30.

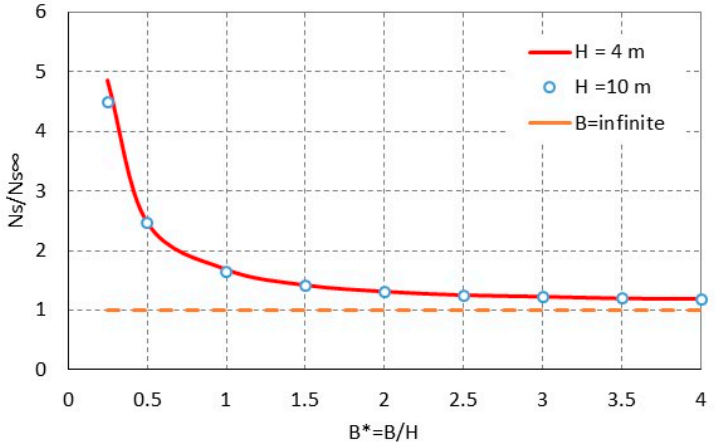

Figure 6. Comparison of the model validity for different sizes of the reference model. Case: Friction angle $\phi' = 30$.

The soil is assumed to have perfect elastoplastic behavior, with the Mohr-Coulomb failure criterion characterized by the internal friction angle ϕ' and the effective cohesion c'. This method is generally utilized for analyzing stability issues without requiring more complex models. A mixed-type soil is considered, the common one that may need the use of the discontinuous support analyzed in this research, being studied the long-term stability only (a purely cohesive soil with high undrained cohesive strength may not need such specific support measures).

3. Results and Discussion

3.1. Rigid Shielded Support

A perfectly rigid shielded support is assumed in this case on the lateral sides of the slope. No friction is assumed on the shield-soil interface.

The N_s results obtained for this configuration are presented in Figure 7, which shows the expected behavior of the supported slope. When increasing the non-supported slope width B, stability significantly reduces, approaching the behavior of the infinite slope. When the value of B is reduced to a level comparable to the slope height H (specifically when $B/H = 1$), stability increases significantly. This is due to the arching effect that occurs between the soil and the supports, which will be explained in the next section. This finding demonstrates that discontinuous support is an effective solution for excavating unstable soils.

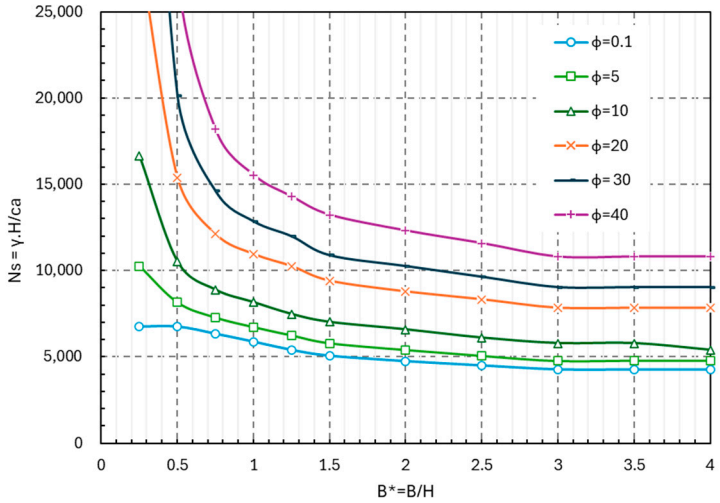

Figure 7. Stability results for rigid shield-supported slope.

Figure 8 presents the normalized results by the infinite slope stability number $N_s/N_{s\infty}$. Though Figure 7 is undoubtedly helpful in estimating slope stability, Figure 9 offers more insight into physical behavior. Figure 8a highlights three distinct stability ranges: from B/H = 3 to infinity, where results match the 2D findings ($N_s/N_{s\infty}$ = 1); from B/H = 1 to 3, where results are consistent across soil properties; and from B/H = 0 to 1, where stability varies with soil friction angle and the B/H ratio. Detailed observations of the two zones, specifically H/B = 0 to 1 and H/B = 1 to 3, can be found in the expanded Figure 8b.

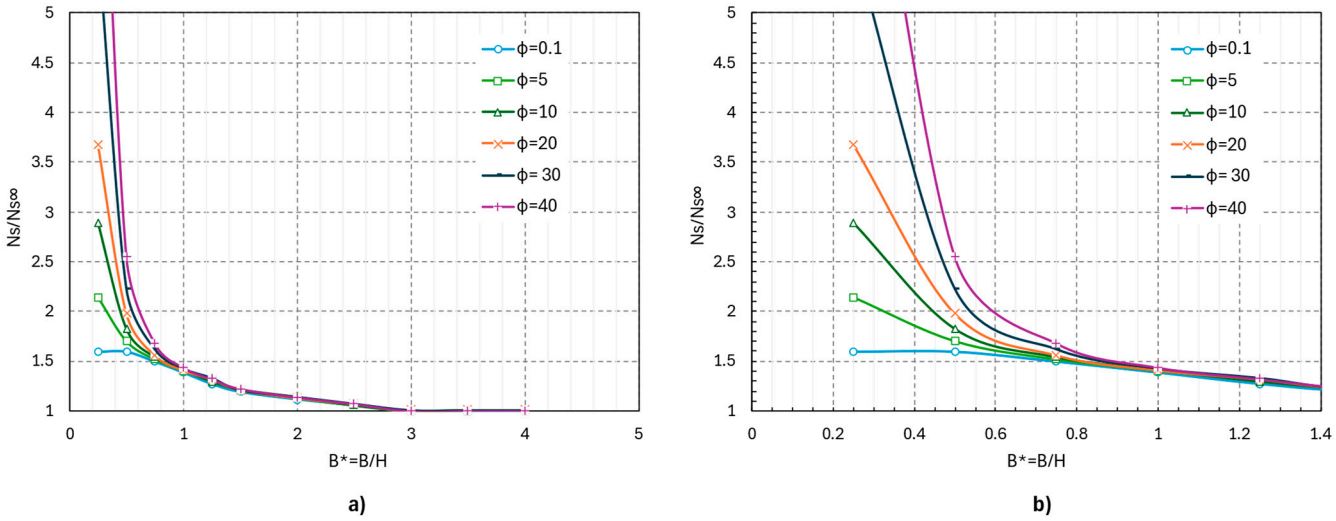

Figure 8. Normalized stability results in a rigid shield-supported slope. (**a**) Range B/H 0 to 5 (**b**) Expanded range 0 to 1.4.

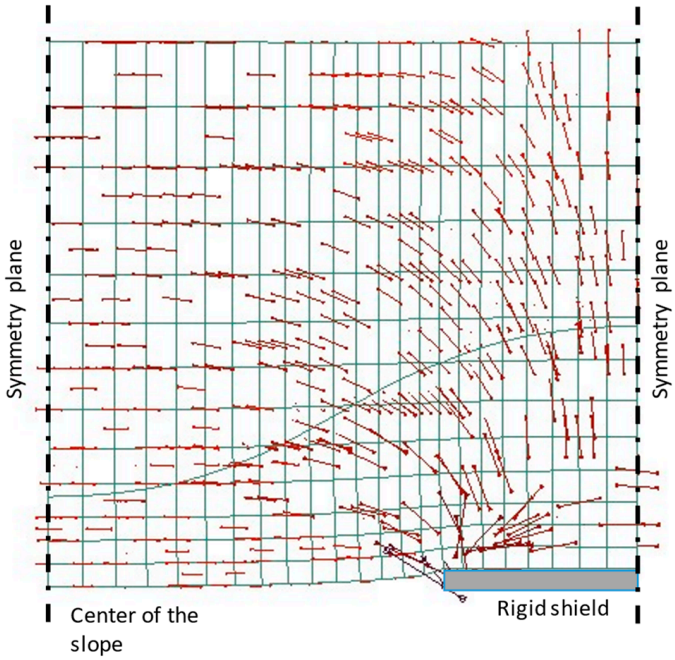

Figure 9. Plan view of the arching effect represented by the middle principal stress in the soil σ_2. Case: Friction angle ϕ' = 30, c' = 20 kN/m^2, B = 6 m. Horizontal cut of the slope at 3 m over the slope foot.

This difference between parts is due to the relative importance of the soil weight and the contribution of the lateral support to the slope stability in each of them. For higher H/B values, the lateral support does not contribute much to general stability, the resistance depending on the shear stress developed along the slip circle, obtaining a $N_s/N_{s\infty}$ ratio

near 1. This situation changes for smaller B/H ratios, increasing the $N_s/N_{s\infty}$ ratio with the friction angle of the soil.

This differentiation greatly helps to develop a practice procedure since it reduces the complexity of determining the slope safety factor to the third part (H/B = 0 to 1).

Construction practice can directly use these ratios to define the stable slope width (B) supported by shields, for a given slope height (H). This categorization simplifies the practical process of determining the slope safety factor by focusing on the third range (H/B = 0 to 1). For this specific part, the stability number changes dramatically with the soil angle of friction and requires a close study. In all the other cases, the curve behavior is almost identical, regardless of the soil properties.

3.2. Arching Effects

The "arch effect" in soils refers to a phenomenon that occurs when soil forms an arch-like structure due to pressure distribution. This effect typically happens when forces applied to a granular material cause the particles to interlock or form a stable arch, allowing the material to support weight without directly transferring it through the entire mass. The arching effect produced by the discontinuous-supported slopes causes a redistribution of stress in the body of the soil due to the restriction to its natural movement imposed by the lateral supports. This effect enhances the slope stability and, at the same time, increases the stress and pressure on the supporting structure. The friction between particles deviates the second principal stress towards the rigid shields, as shown in Figure 9.

The influence of the arching effect produces a reduction in the horizontal displacement of the slope, characterizing the same phenomenon and correlating with the same three B/H zones distinguished in the previous section. The horizontal displacement is less important as the free slope width B increases, reaching a point where the center top of the slope moves without restriction. In this case, slope stability equals that of the unshielded case. Figure 10 shows this variation. Comparing these results with those in Figure 9, one can see that by increasing B/H from 3, the influence of the supports is minimal, resulting in a stability number very close to the asymptote of value 1 in Figure 9 (infinite slope). From value B/H = 2 to B/H = 1 there is an important reduction in u_x (Figure 11), which means a significant increase in N_s/N_∞ (Figure 9).

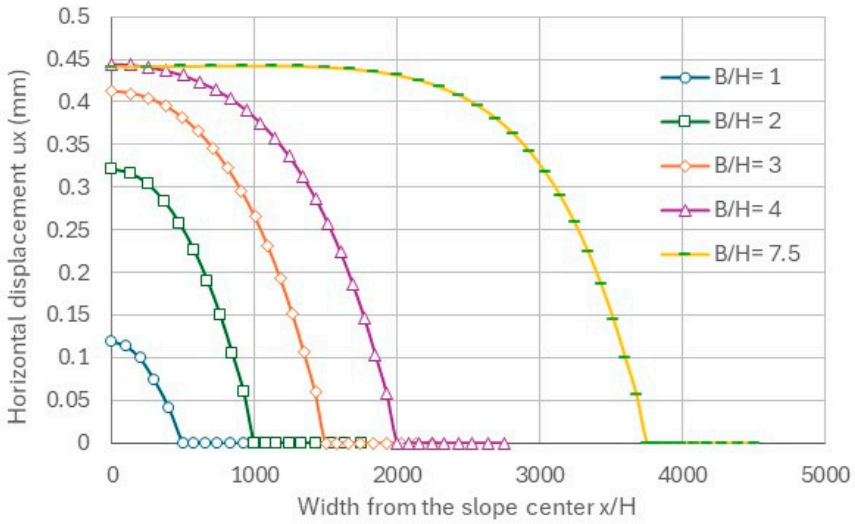

Figure 10. Variation of the horizontal displacement of the center top of the slope for different slope widths.

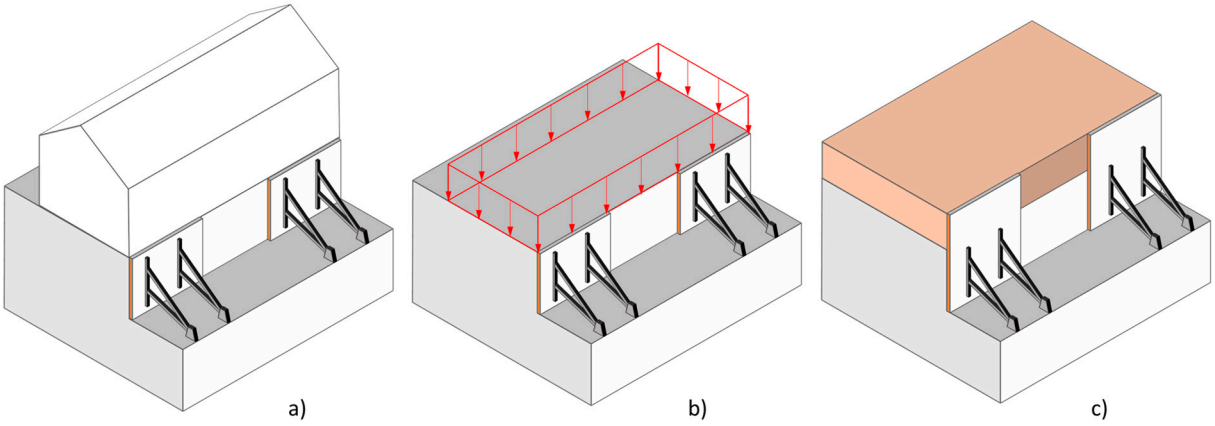

Figure 11. Simplified procedure to consider a load over the top of the slope. (**a**) Actual excavation near a building (**b**) Load equivalent to the building (**c**) Soil stratum added to the initial excavation to study slope stability.

3.3. Consideration of Loads Adjacent to the Slope

In urban environments, excavation is usually constructed near a street, road, or building, being crucial to ensure sustainability factors, especially those related to economic and environmental sustainability, including risk reduction because it increases the likelihood of damage. The impact of these nearby structures on slope stability can be directly assessed using the previously developed model.

It is important to note that the proposed model only assesses slope stability and does not include deformation control to address induced settlement on nearby structures, which is outside the scope of this research. Future studies will consider different models to adequately represent deformations, adding some other models with more complexity to the basic elastic behavior.

The most common method used in practice when the load is extended over the whole top of the slope (or this conservative hypothesis is adopted) is to add an equivalent soil stratum to slope height that produces the same increase of stress in the soil as the substituted load. Figure 11 provides a schematic representation of the calculation process.

Consequently, the slope with a load q on top will be directly changed by a slope with a new height equal to $H^* = H + q/\gamma$, where H and H^* are the original and the corrected height, and γ is the soil self-weight.

The use of the proposed calculation charts is then straightforward, considering the variables B/H^* and $N_s/N_{s\infty}{}^*$, where the superscript (*) refers to the variables calculated using the corrected height H^*.

3.4. Worked Example

A practical example is provided below to aid in using the charts for calculations.

Consider an excavation of 3.5 m in soil with a friction angle of $\phi' = 20^\circ$ and cohesive strength $c' = 10$ kN/m^2. A load of 20 kN/m^2 is applied on top of the slope. To obtain the maximum shield separation with a safety factor of $F = 1.5$, we use the chart in Figure 8 if no deformation is considered in the shield.

The equivalent infinite slope can be calculated using common software, considering the previous problem data, but with $H^* = H + q/\gamma = 4.5$ m. This calculation gives a safety factor of $F_{s\infty}{}^* = 0.71$, and then $N_s/N_{s\infty}{}^* = F_s/F_{s\infty}{}^* = 1.5/0.71 = 2.11$.

Taking the previous value at the vertical axis in Figure 8 and drawing a horizontal line towards the $\phi' = 20^\circ$ curve, the intersection gives the corresponding B/H^* value. The procedure is presented in Figure 12.

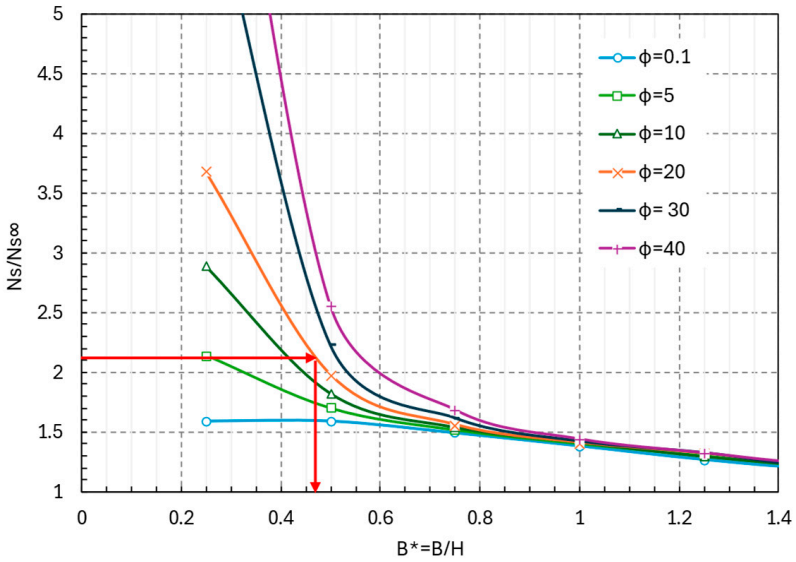

Figure 12. Example procedure for practical calculation of the discontinuous supported slope.

From the graphical procedure in Figure 12 the ratio $B/H^* = 0.46$, and consequently, $B = 0.46 \times 4.5 = 2.1$ m, which is the maximum open slope for a safe excavation with $F = 1.5$.

It is important to note that the proposed methodology assumes some simplifying hypotheses that require proper consideration for each case, including homogeneous soil and perfect elastoplastic behavior.

4. Conclusions

This research presents a study on the stability of discontinuously supported slopes, which are very common in practice but receive limited attention in the literature and only partial references in professional codes.

The main results obtained from the research are:

1. The behavior of a slope with discontinuous support is analyzed, presenting a model that characterizes its performance and allows for the calculation of its safety.
2. A novel, easy-to-use procedure based on normalized charts is presented to check discontinuously supported slopes with a specific safety factor.
3. Normalization using the ratio $N_s/N_{s\infty}$ helps clarify the behavior of the supported slope. It reveals that all lines associated with different soil properties converge to a single line, diverging only at specific values of B/H where the arching effect becomes significant. This normalization also simplifies the calculation. All the slopes behave almost identically when $B/H > 1$, only diverging for very small widths.
4. Since there is no established method to check the safety of shallow discontinuous-supported excavation, the sustainability of excavation work in building construction can be enhanced by the proposed method. By adopting this procedure, we can promote a safer and more environmentally responsible excavation process that prioritizes the safety of workers and decreases the likelihood of damage to nearby structures.
5. This research supports Sustainable Development Goal 11—promoting inclusive, safe, resilient, and sustainable cities—by providing an accessible safety analysis method for discontinuously supported shallow excavations that does not require expertise in complex numerical models.

Author Contributions: Conceptualization, M.A.M.; methodology, M.A.M.; software, M.A.M., D.M.-C. and A.C.; validation, M.A.M.; resources, D.M.-C. and A.C.; writing—original draft preparation, M.A.M.; writing—review and editing, M.A.M. and D.M.-C. All authors have read and agreed to the published version of the manuscript.

Funding: This research received no external funding.

Institutional Review Board Statement: Not applicable.

Informed Consent Statement: Not applicable.

Data Availability Statement: Dataset available on request from the authors.

Conflicts of Interest: The authors declare no conflicts of interest.

References

1. Ministry of Housing. ORDER of 1 March 1976, Norma Tecnológica de la Edificación NTE-ADV/1976, «Acondicionamiento del terreno. Desmontes: Vaciado» BOE 6 March 1976 and 13 March 1976, no. 57 and 63. Available online: https://www.boe.es/boe/dias/1976/03/06/pdfs/R04700-05230.pdf (accessed on 23 November 2024).
2. *BS 6031:2009*; Civil Engineering and Building Structures Standards Committee. BS British Standards: London, UK, 2009. Available online: https://geotechnicaldesign.info/bs6031-2009.html (accessed on 23 November 2024).
3. *DIN 4124:2012-01*; Excavations and trenches—Slopes, Planking and Strutting Breadths of Working Spaces. Deutsches Institut für Normung: Berlin, Germany, 2012.
4. Rotaru, A.; Bejan, F.; Almohamad, D. Sustainable Slope Stability Analysis: A Critical Study on Methods. *Sustainability* **2022**, *14*, 8847. [CrossRef]
5. Azarafza, M.; Akgün, H.; Ghazifard, A.; Asghari-Kaljahi, E.; Rahnamarad, J.; Derakhshani, R. Discontinuous rock slope stability analysis by limit equilibrium approaches—A review. *Int. J. Digit. Earth* **2021**, *14*, 1918–1941. [CrossRef]
6. Hisham, T.E. Two- and three-dimensional analyses of translational slides in soils with nonlinear failure envelopes. *Can. Geotech. J.* **2010**, *47*, 388–399. [CrossRef]
7. Hisham, T.E.; Azza, M.E.; Hazem, G.E.; Amani, G.S. Stability analysis and charts for slopes susceptible to translational failure. *Can. Geotech. J.* **2006**, *43*, 1374–1388. [CrossRef]
8. Zhang, Y.; Chen, G.; Zheng, L.; Li, Y.; Zhuang, X. Effects of geometries on three-dimensional slope stability. *Can. Geotech. J.* **2013**, *50*, 233–249. [CrossRef]
9. Ho, I.H. Parametric Studies of Slope Stability Analyses Using Three-Dimensional Finite Element Technique: Geometric Effect. *J. GeoEng.* **2014**, *9*, 33–43. [CrossRef]
10. Nian, T.K.; Huang, R.Q.; Wan, S.S.; Chen, G.Q. Three-dimensional strength-reduction finite element analysis of slopes: Geometric effects. *Can. Geotech. J.* **2012**, *49*, 574–588. [CrossRef]
11. Griffiths, D.V.; Marquez, R.M. Three-dimensional slope stability analysis by elasto-plastic finite elements. *Géotechnique* **2007**, *57*, 537–546. [CrossRef]
12. Samadhiya, V.; Chavda, J.T. Numerical Investigations on Stability of 3D Soil Slopes with Different Boundary Conditions. *Indian Geotech J.* **2024**, *54*, 1341–1365. [CrossRef]
13. Gourvenec, S.; Powrie, W. Three-dimensional finite element analysis of embedded retaining walls supported by discontinuous earth berms. *Can. Geotech. J.* **2001**, *37*, 1062–1077. [CrossRef]
14. Powrie, W.; Daly, M.P. Centrifuge model tests on embedded retaining walls supported by earth berms. *Geotechnique* **2002**, *52*, 89–106. [CrossRef]
15. Smethurst, J.A.; Powrie, W. Effective-stress analysis of berm-supported retaining walls. *Proc. Inst. Civ. Eng.-Geotech. Eng.* **2008**, *161*, 39–48. [CrossRef]
16. Liao, H.-J.; Lin, C. Case studies on bermed excavation in Taipei silty soil. *Can. Geotech. J.* **2009**, *46*, 889–902. [CrossRef]
17. Sabzi, Z.; Fakher, A. 3D Response of an Excavation Adjacent to Buildings Supported by Inclined Struts. *Acta Geotech. Slov.* **2017**, *14*, 39–53. Available online: https://dk.um.si/IzpisGradiva.php?lang=eng&id=70884 (accessed on 23 September 2024).
18. Cano, M.; Pastor, J.L.; Miranda, T.; Tomás, R. Procedimiento constructivo de muros de sótano mediante bataches con juntas de conexión. Estudio del ancho óptimo de excavación en suelos mixtos. *Inf. Construcc.* **2020**, *72*, e344. [CrossRef]
19. Cano, M.; Pastor, J.L.; Riquelme, A.; Tomás, R. Design stability charts for construction procedure of basement walls using staged bermed excavation: A parametric study. *Can. Geotech. J.* **2024**. [CrossRef]
20. Duncan, J.M.; Wright, S.G. *Soil Strength and Slope Stabilty*; John Wiley & Sons, Inc.: Hoboken, NJ, USA, 2005; p. 199.
21. *Abaqus v 2018*; Dassault Systemes Simulia Corporation: Providence, RI, USA, 2018.
22. ABAQUS Analysis User's Manual. Chapter 18.3.3 Mohr-Coulomb Plasticity. Available online: https://classes.engineering.wustl.edu/2009/spring/mase5513/abaqus/docs/v6.6/books/usb/default.htm?startat=pt05ch18s03abm30.html#usb-mat-cmohrcoulomb (accessed on 23 October 2024).